Xi'an Shiyou Daxue Xuebao (Ziran Kexue Ban)/
Journal of Xi'an Shiyou University, Natural Sciences Edition
ISSN: 1673-064X
E-Publication: Online Open Access
Vol: 67 Issue 11 | 2024
DOI: 10.5281/zenodo.14195656

MODELING WITH PREDICTION OF BURST PRESSURE OF ELLIPTICAL CORRODED PIPELINE

AICHA METEHRI *
University of Sidi Bel Abbes, Faculty of Technology, Department of Mechanical Engineering, Laboratory of Mechanics Physical of Material (LMPM), 22000, Algeria.
*Corresponding Author Email: ametehri@yahoo.com

BELAID MECHAB
University of Sidi Bel Abbes, Faculty of Technology, Department of Mechanical Engineering, Laboratory of Mechanics Physical of Material (LMPM), 22000, Algeria. Email: bmechab@yahoo.fr

BEL ABBES BACHIR BOUADJRA
University of Sidi Bel Abbes, Faculty of Technology, Department of Mechanical Engineering, Laboratory of Mechanics Physical of Material (LMPM), 22000, Algeria. Email: bachirbou@yahoo.fr

Abstract

The objective of this study is to develop a new model predicting the burst pressure of an elliptical defect in a corroded pipe under internal pressure. The effects of geometric parameters on the pipeline performance were analyzed. The results of our analytical model were compared with those of the well-known LPC model for unrepaired corroded pipes, and there is a good agreement between the two models. For the corroded steel pipe, the comparison between the newly developed model and finite element (FE) calculations also showed a good agreement.

Index Terms: Modeling**,** Burst pressure**,** Pipeline, Corrosion, Steel, FE.

1. INTRODUCTION

Pipelines are of paramount significance within the energy infrastructure, enabling the efficient conveyance of gas, oil, and diverse hydrocarbons across extensive distances to meet the needs of the petrochemical sector [1]. These pipeline systems typically comprise multiple sections composed of wide-diameter, thin-walled carbon steel pipes, often operating under substantial internal pressure [2-4]. The burst pressure of these pipelines plays a pivotal role in determining the material selection, structural design, safe operational practices, and integrity assessment [5].

For over five decades, predictive models for the burst pressure of cylindrical vessels and pipes have been under development. The aim is to quantify the maximum pressure at which failure may occur based on material characteristics, as well as the dimensions of the vessel or pipe [6, 7]. Corrosion imperfections can be found in pipelines of various sizes, configurations, and orientations. Corrosion poses the risk of potentially catastrophic failures in pipelines and is acknowledged as a major concern for the safety and structural integrity of both onshore and offshore pipeline systems [8, 9].

Corrosion represents a defect that has a significant impact on the performance of pipelines and contributes to a decrease in their lifespan and efficiency in delivering

ISSN: 1673-064X
E-Publication: Online Open Access
Vol: 67 Issue 11 | 2024
DOI: 10.5281/zenodo.14195656

essential natural resources to consumers [10]. The behavior of pipelines affected by corrosion remains the subject of ongoing research [11]. [12, 13] models provided the best prediction in their original form without being calibrated.

In the literature, models predicting burst pressure in pipelines are very rare; this prompted us to carry out this research to develop an analytical model enabling this prediction to facilitate the design of corroded pipe. This study also presents a finite element analysis describing the effects of the various parameters influencing the performances of pipes. All these parameters were introduced into the developed analytical model.

2. GEOMETRICAL MODEL

In this study, we suppose the existence of a corrosion defect of elliptical shape in the central outer wall of a pipeline. The dimensions of the defect are: radius R= 20mm, and the depth is d=8.5mm. The outside diameter of the pipe De is 600 mm, ‘’Di’’ represents the inside diameter (Di = 580 mm), and "t" designates the pipe thickness (t = 10 mm). The pipeline is subjected to an internal pressure of P = 8.42 MPa. Figure 1 illustrates the corrosion pipe's geometric characteristics.

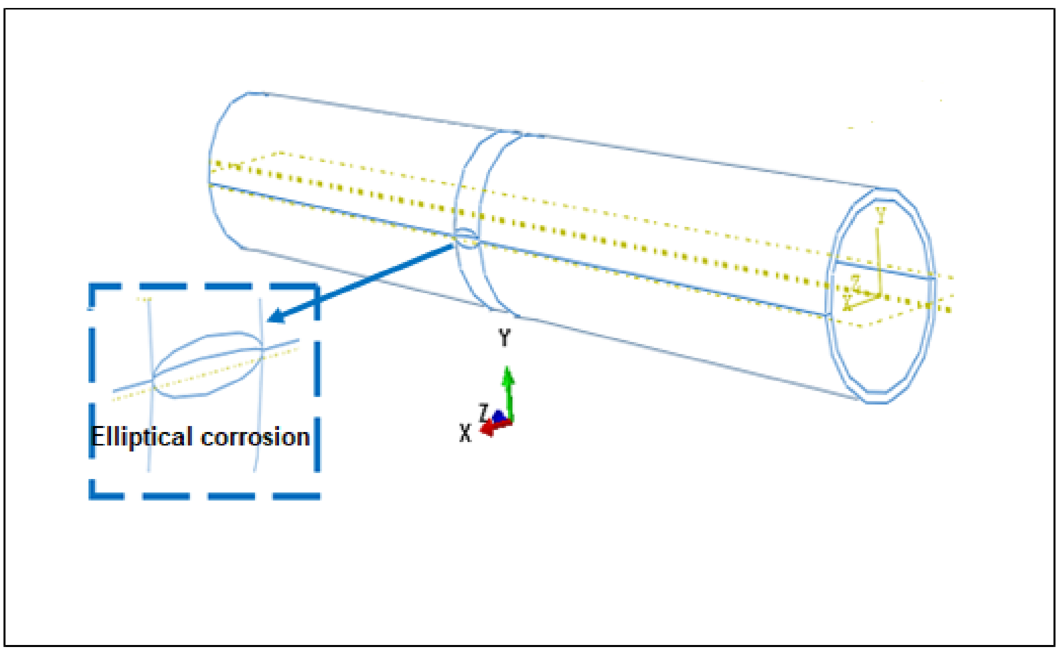

Figure 1: The corrosion pipe's geometric characteristics

We used a material commonly used in the fuel transportation industry that is robust to mechanical, thermal, and various environmental and application requirements. The table below shows the characteristics of the API 5L X65 steel we used. The elastic properties of the pipe are shown in Table 1. The pipe steel is supposed to have an elastic-plastic behavior.

ISSN: 1673-064X
E-Publication: Online Open Access
Vol: 67 Issue 11 | 2024
DOI: 10.5281/zenodo.14195656

Table 1: Mechanical properties of steel material used in this study

Properties	Steel X65 [14]
E (GPa)	211
ν	0.3
σ_{uts} (MPa)	500
σ_e (MPa)	380
n	0.127

3. INITIAL CONDITIONS AND LIMITATIONS

The ends of the pipe were constrained (All displacements and rotation were blocked) for the calculation to run smoothly, and the length of the pipe section was chosen so that this recessing would not influence the stress calculations in the corroded and repaired area of the pipe. The pipe is subjected to an internal pressure of 8.42 MPa. (The boundary conditions are presented in Figure 2).

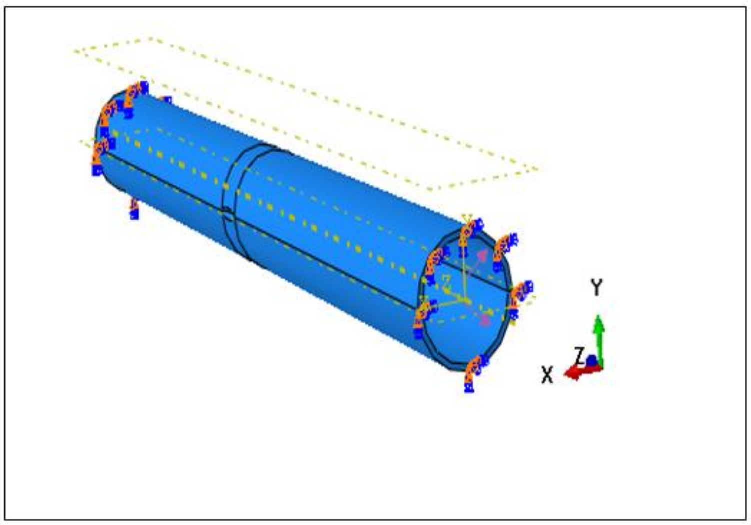

Figure 2: Boundary condition of the elliptical corroded pipe

4. FEM MODEL

The ABAQUS calculation code [15] was used to calculate the equivalent and the normal stresses in the elliptical corroded pipeline. In terms of mesh type, we opted for elements (C3D10), which have been frequently used in the modeling of such structures. It is also important to refine the mesh at a defect level to better determine the value of the normal stresses. The general configuration is based on a regular mesh, which is kept constant for all the analyses carried out in this study to avoid any influence of the mesh on the results. The total number of elements is about 20131. The total number of nodes is 39485. Figure 3 illustrates the structure of the mesh employed for this calculation.

ISSN: 1673-064X
E-Publication: Online Open Access
Vol: 67 Issue 11 | 2024
DOI: 10.5281/zenodo.14195656

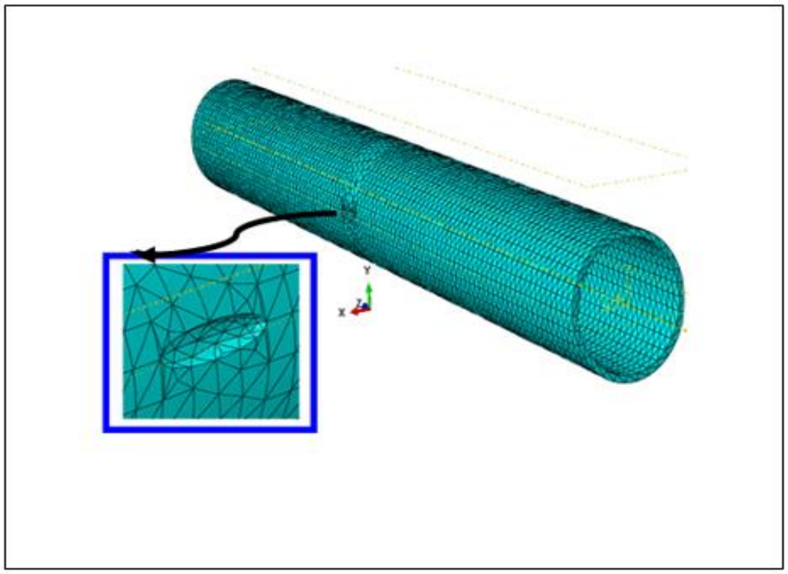

Figure 3: Full mesh employed for numerical model of the defective pipe

5. RESULTS AND DISCUSSION

5.1 Equivalent and Normal Stresses Results

This study obtained figures representing the equivalent and normal stresses in the case of an unrepaired pipe with elliptical defect. The results are presented in Figure 4.

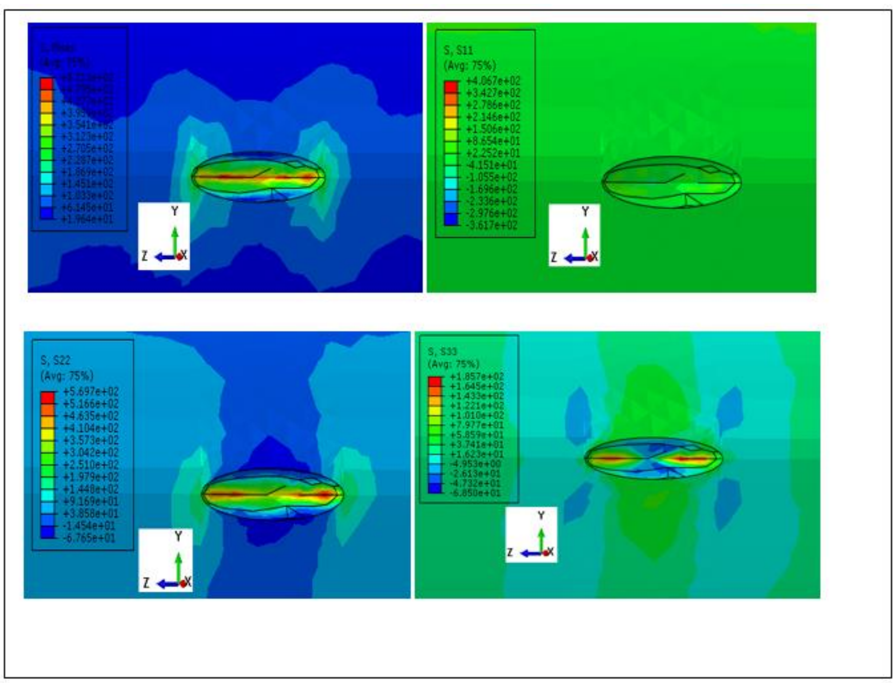

Figure 4: Equivalent and Normal stresses for elliptical corrosion

Xi'an Shiyou Daxue Xuebao (Ziran Kexue Ban)/
Journal of Xi'an Shiyou University, Natural Sciences Edition
ISSN: 1673-064X
E-Publication: Online Open Access
Vol: 67 Issue 11 | 2024
DOI: 10.5281/zenodo.14195656

The von -Mises and normal stress levels for one example of our model are shown in the results above, and we can see that:

- Concentration of the equivalent and normal stresses situated at the defect's corners.
- It can reach $>$ 500 MPa for the equivalent and a hoop stresses, a value almost superior to the ultimate stress of steel used in this study (see table 1).
- This value of Hoop stress (S22) leads to damage to pipeline gas transportation. The radial (S11) and the longitudinal (S33) stresses present no risk of bursting the pipe.
- The elliptical corrosion presents a very high level, corresponding to just 8.42 MPa internal pressure.*r*2

6. ANALYTICAL MODEL FOR ELLIPTICAL CORROSION PIPE

6.1 LPC Model

Based on a large number of elastic-plastic Finite Element Analysis (FEA) results and burst test data X65 a corroded pipeline, a line pipe corrosion (LPC) model was developed at British Gasin [10, 16] to determine the burst pressure of corroded thin-walled pipes. The burst pressure in this model was expressed as follows:

$$P_{bi} = \frac{2t\sigma_{uts}}{(D-t)} \tag{3}$$

$$P_b = \frac{2t\sigma_{uts}}{(D-t)}\left(\frac{L}{\sqrt{Dt}}\right)^{\eta}.H \quad For \quad 0.1 \le \frac{L}{\sqrt{Dt}} \le 12 \quad ,0.2 \le \frac{d}{t} \le 0.8 \tag{4}$$

η = 0.127

η and H functions are given by the following formulae: With three values for d/t = 0.2, 0.5 and 0.8.

$$\begin{cases} \eta = 0.05067 - 0.55833\left(\dfrac{d}{t}\right) - 1.115\left(\dfrac{d}{t}\right)^2 \\ H = 0.89683 + 0.52383\left(\dfrac{d}{t}\right) - 0.05\left(\dfrac{d}{t}\right)^2 \end{cases} \tag{5}$$

Xi'an Shiyou Daxue Xuebao (Ziran Kexue Ban)/
Journal of Xi'an Shiyou University, Natural Sciences Edition
ISSN: 1673-064X
E-Publication: Online Open Access
Vol: 67 Issue 11 | 2024
DOI: 10.5281/zenodo.14195656

Table 2: Comparison of the present model (1) with LPC model, for different d/t ratios d/t=0.2; 0.5 and d/t=0.8

	0≤L/(Dt)^0.5≤12								
	d/t=0.2			d/t=0.5			d/t=0.8		
L/(Dt)^0.5	**Pb/Pbi (Present)**	**Pb/Pbi (LPC)**	**e (%)**	**Pb/Pbi (Present)**	**Pb/Pbi (LPC)**	**e (%)**	**Pb/Pbi (Present)**	**Pb/Pbi (LPC)**	**e (%)**
0,44721	1,00676	0,99265	1,42145	1,02	0,97122	5,0225	0,84994	0,89404	-4,93267
1	0,957	0,96939	-1,2781	0,88	0,88787	-0,8863	0,60229	0,66437	-9,34419
1,41421	0,93633	0,94914	-1,3496	0,80948	0,8235	-1,7024	0,51927	0,53842	-3,5567
2	0,91611	0,92339	-0,7884	0,74462	0,75084	-0,8284	0,44768	0,42967	4,19159
3,16228	0,89005	0,88768	0,26699	0,66678	0,66395	0,42624	0,36797	0,33063	11,29359
4	0,87697	0,87139	0,64036	0,63007	0,62878	0,20516	0,33276	0,29748	11,85962
5	0,86472	0,85801	0,78204	0,59708	0,60171	-0,7694	0,30245	0,27414	10,32684
6	0,85485	0,84867	0,7282	0,57141	0,58369	-2,1038	0,27975	0,25954	7,78685
6,9282	0,84714	0,84227	0,5782	0,55194	0,57174	-3,4631	0,26304	0,25024	5,11509
8	0,8395	0,83665	0,34064	0,53314	0,5615	-5,0507	0,24734	0,2425	1,99588
9,48683	0,83053	0,83091	-0,0457	0,51168	0,55127	-7,181	0,22994	0,23497	-2,1407
10	0,82778	0,82932	-0,1856	0,50523	0,54848	-7,8854	0,22481	0,23294	-3,49017
10,48809	0,8253	0,82795	-0,3200	0,49946	0,54609	-8,5388	0,22027	0,23122	-4,73575
10,95445	0,82304	0,82675	-0,4487	0,49425	0,54401	-9,1468	0,21621	0,22974	-5,88927
11,40175	0,82097	0,8257	-0,5728	0,4895	0,54218	-9,7163	0,21254	0,22844	-6,96025
12	0,81833	0,82441	-0,7375	0,48351	0,53996	-10,455	0,20793	0,22686	-8,34435

Figure 5 presents a comparison between our first model and the LPC one for unrepaired corroded pipe. It can be noted that the two curves of the burst pressure of the present first model with the LPC model have points that are almost close and the difference is almost negligible for all ratios of defect d/t=0.2, 0.5 and 0.8 (see table 2). This result confirms the validation of our model. On the other hand, the burst pressure decreases with the increase of the geometrical ratio (d/t) of the corroded pipe. We can also see that the ratio Pb/Pbi exhibits an asymptotic behavior as the ratio L/ (DT) 0.5 increases. The asymptotic values depend; the asymptotic value of this ratio depends on the geometrical ratio d/t.

ISSN: 1673-064X
E-Publication: Online Open Access
Vol: 67 Issue 11 | 2024
DOI: 10.5281/zenodo.14195656

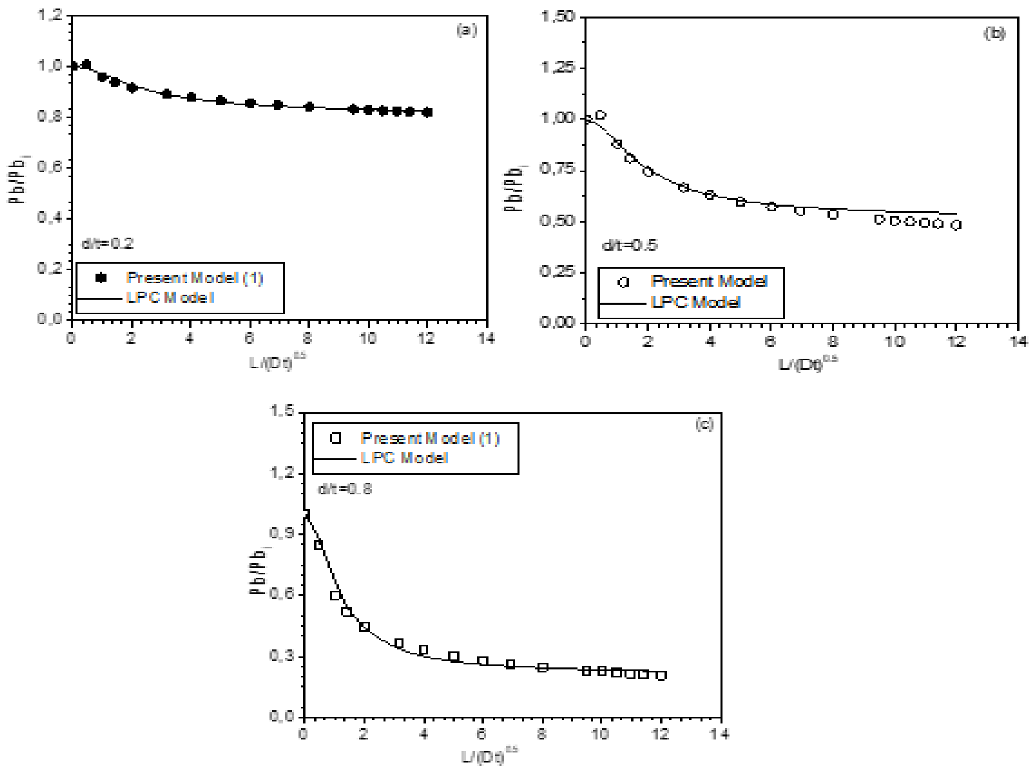

Figure 5: Comparison of the present model (1) of unrepaired pipe with LPC model for d/t=0.2, 0.5 and 0.8 respectively

6.2. Second Model (2)

In the second model, the burst pressure was modeled as the exponential function as a function of the ratio L/ (Dt) 0.5 for corroded thin-walled pipes. Three values of the ratio d/t were taken and this model was also compared with the LPC one. In this model, the burst pressure is expressed as follows:

$$P_{bi} = \frac{2t\sigma_{uts}}{(D-t)} \tag{6}$$

$$P_b = \frac{2t\sigma_{uts}}{(D-t)}\left(A_0 + A_1 \exp\left(A_2\left(\frac{L}{\sqrt{Dt}}\right)\right)\right) \quad For \quad 0 \le \frac{L}{\sqrt{Dt}} \le 12 \quad ,0.1 \le \frac{d}{t} \le 0.8 \tag{7}$$

$$A_0 = -0{,}1078\left(\frac{d}{t}\right)^2 - 0{,}8697\left(\frac{d}{t}\right) + 0{,}99805$$

$$A_1 = -0{,}02192\left(\frac{d}{t}\right)^2 + 0{,}94688\left(\frac{d}{t}\right) - 6{,}46667.10^{-4} \tag{8}$$

$$A_2 = -0{,}82048\left(\frac{d}{t}\right)^2 + 0{,}22829\left(\frac{d}{t}\right) - 0{,}29502$$

Xi'an Shiyou Daxue Xuebao (Ziran Kexue Ban)/
Journal of Xi'an Shiyou University, Natural Sciences Edition
ISSN: 1673-064X
E-Publication: Online Open Access
Vol: 67 Issue 11 | 2024
DOI: 10.5281/zenodo.14195656

Table 3: Comparison of the present model (2) with LPC model for different d/t ratios d/t=0.2; 0.5 and 0.8

	0≤L/(Dt)^0.5≤12								
	d/t=0.1			**d/t=0.5**			**d/t=0.8**		
L/(Dt)^0.5	**Pb/Pbi (Present)**	**Pb/Pbi (LPC)**	**e(%)**	**Pb/Pbi (Present)**	**Pb/Pbi (LPC)**	**e(%)**	**Pb/Pbi (Present)**	**Pb/Pbi (LPC)**	**e(%)**
0	1,00426	1	-0,4262	1,01453	1	-1,4525	1,00418	1	-0,41841
1	0,98121	0,98616	0,5015	0,86138	0,88787	2,98391	0,64082	0,66437	3,5446
1,41421	0,97341	0,97674	0,34136	0,81334	0,8235	1,23383	0,54625	0,53842	-1,4549
2	0,9638	0,96444	0,06616	0,75727	0,75084	-0,8561	0,44873	0,42967	-4,43633
3,16228	0,94884	0,94676	-0,2196	0,67737	0,66395	-2,0218	0,33599	0,33063	-1,62208
4	0,94071	0,93844	-0,2417	0,63839	0,62878	-1,5277	0,2935	0,29748	1,33671
5	0,9332	0,93149	-0,1836	0,60568	0,60171	-0,6600	0,26513	0,27414	3,2884
6	0,92753	0,92657	-0,1034	0,58345	0,58369	0,04119	0,25012	0,25954	3,62827
6,9282	0,92351	0,92317	-0,0370	0,56924	0,57174	0,43761	0,24261	0,25024	3,04946
8	0,92001	0,92016	0,01683	0,55806	0,5615	0,61215	0,238	0,2425	1,85567
9,48683	0,91659	0,91706	0,05071	0,54854	0,55127	0,4954	0,23512	0,23497	-0,06406
10	0,91571	0,9162	0,05333	0,54633	0,54848	0,39176	0,23461	0,23294	-0,7178
10,48809	0,91498	0,91545	0,05122	0,5446	0,54609	0,27273	0,23426	0,23122	-1,31506
10,95445	0,91437	0,9148	0,04692	0,54323	0,54401	0,14422	0,23401	0,22974	-1,85998
11,40175	0,91386	0,91423	0,04093	0,54212	0,54218	0,01111	0,23384	0,22844	-2,36198
12	0,91326	0,91352	-0,0028	0,54091	0,53996	0,00704	0,23367	0,22686	0,1635

Figures 6 (b and c) present the comparison of the present second model (2) with the LPC model for different d/t ratios (a) d/t=0.2; (b) d/t=0.5 and (c) d/t=0.8. We note that the burst decreases in the burst pressure result in an increase when the ratio L/ (Dt) 0.5 is lower than 4. After this value, the burst pressure exhibits an asymptotic behavior. The results show a good agreement between our second model (2) and the LPC one for different defect ratios of defect d/t, the difference does not exceed 3.62% (see table 3).

Xi'an Shiyou Daxue Xuebao (Ziran Kexue Ban)/
Journal of Xi'an Shiyou University, Natural Sciences Edition
ISSN: 1673-064X
E-Publication: Online Open Access
Vol: 67 Issue 11 | 2024
DOI: 10.5281/zenodo.14195656

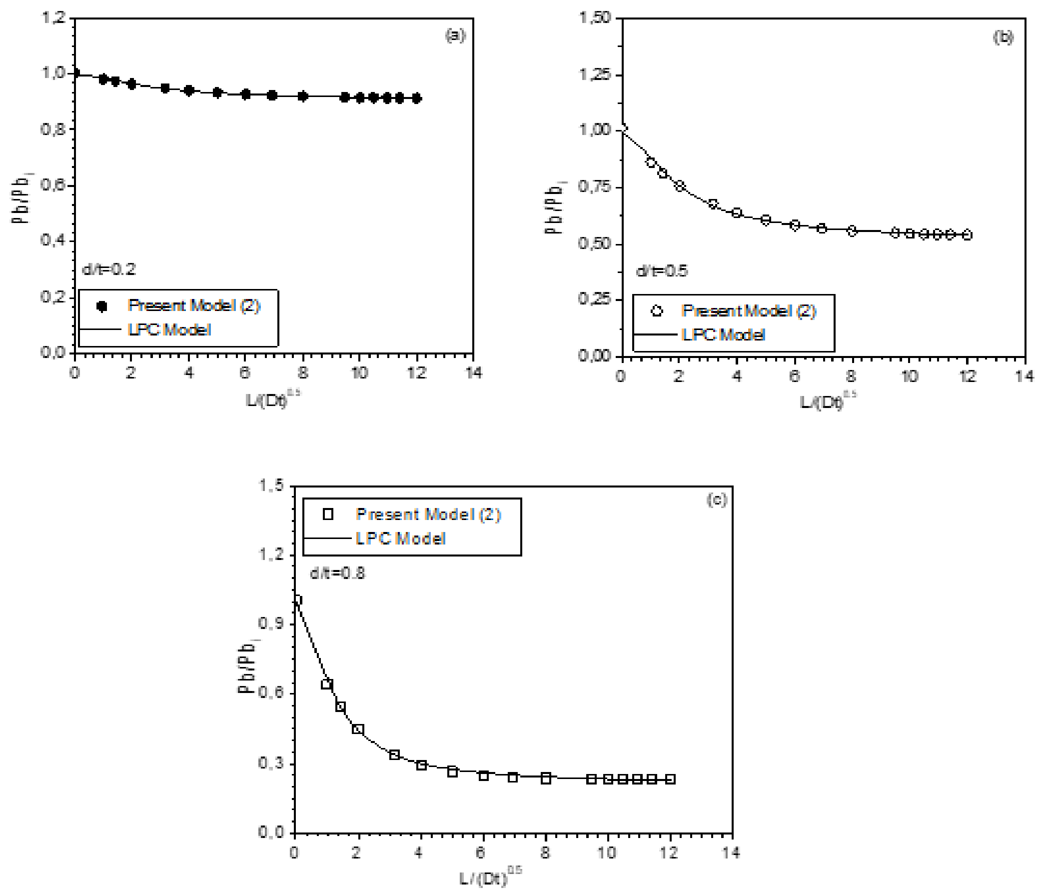

Figure 6: Comparison of the present second model (2) of unrepaired pipe with LPC model for d/t=0.2, 0.5 and 0.8 respectively

7. CONCLUSION

This study aimed to use the finite element method to develop an analytical model predicting the burst pressure in a corroded pipe. The finite element calculation showed that this pressure depends on the elastic properties and geometrical parameters of the pipe. The various parameters influencing the burst pressure of the pipe were introduced into the model for estimating this pressure. So, while choosing a model, you must be careful about the pipe's geometry and material characteristics. The comparison between the results of our model analytic and those obtained using finite elements showed very good agreement.

NOMENCLATURE

FEM:	Finite element method
σeq:	von-Mises equivalent stress
S22:	Hoop stress

ISSN: 1673-064X
E-Publication: Online Open Access
Vol: 67 Issue 11 | 2024
DOI: 10.5281/zenodo.14195656

σuts:	The ultimate stress.
σe:	Yield stress
A0, A1 and A2:	Integration functions.
d:	Depth defect (mm)
L:	Defect length (mm)
De:	Pipe external diameter (mm)
Di:	Pipe internal diameter (mm)
E:	Young's modulus of steel.
n:	Work hardening coefficient
LPC:	Line pipe corrosion model.
P:	Internal pressure.
Pb:	The burst pressure.
r=d/t:	Geometrical ratio of defect.
t:	Pipe thickness (mm)
η:	Function depend Ratio of defect.
ν :	Poisson's Ratio.

References

1) Mechab B, Serier B, Kaddouri.K; Bachir Bouiadjra. B, 2014. Probabilistic elastic-plastic analysis of cracked pipes subjected to internal pressure load, Nuclear Engineering and Design, Vol 275, pp 281-286, DOI: 10.1016/j.nucengdes.2014.05.008.W.-K. Chen, *Linear Networks and Systems.* Belmont, Calif.: Wadsworth, pp. 123-135, 1993. (Book style)

2) Mechab Belaïd, Medjahdi Malika, Salem Mokadem, Serier Boualem, 2020. ''Probabilistic elastic-plastic fracture mechanics analysis of propagation of cracks in pipes under internal pressure'', Frattura ed Integrità Strutturale, 54,202-210; DOI: 10.3221/IGF-ESIS.54.15.

3) Mechab Belaïd, Chioukh Nadji, Mechab Boubaker, Serier Boualem, 2018. ''Probabilistic Fracture Mechanics for Analysis of Longitudinal Cracks in Pipes under Internal Pressure'', J. Fail. Anal. And Preven. 18(6), pp. 1643–1651, Doi: 10.1007/S11668-018-0564-8.

4) Mechab, B., Serier, B., Bachir Bouiadjra, B., Kaddouri, K., Feaugas, X., 2011. "Linear and non-linear analyses for semi-elliptical surface cracks in pipes under bending", Int. J. Pres. Ves. Pip. 88, 57–63. Doi .Org/10.1016/ J.Ijpv P. 2010 .11.001.

5) Fezazi Amina Ismahène, Mechab Belaïd, Salem Mokadem, Serier Boualem, 2021. '' Numerical prediction of the ductile damage for axial cracks in pipe under internal pressure'', Frattura ed Integrità Strutturale, 58, 231-241; DOI: 10.3221/IGF-ESIS.58.17.

6) Muda, M.F., Hashim, M.H.M., Kamarudin, M.K., Mohd, M.H., Tafsirojjaman, T., Rahman, M.A. and Paik, J.K. 2022. Burst pressure strength of corroded subsea pipelines repaired with composite fiber-reinforced polymer patches. Eng. Fail. Anal., 136, 106204. DOI: 10.1016/j.engfailanal.2022.106204.

Xi'an Shiyou Daxue Xuebao (Ziran Kexue Ban)/
Journal of Xi'an Shiyou University, Natural Sciences Edition
ISSN: 1673-064X
E-Publication: Online Open Access
Vol: 67 Issue 11 | 2024
DOI: 10.5281/zenodo.14195656

7) Budhe, S., Banea, M.D. and de Barros, S. 2019. Prediction of Failure Pressure for Defective Pipelines Reinforced with Composite System, Accounting for Pipe Extremities, J Fail. Anal. And Preven., 19, pp. 1832-1843. DOI: 10.1007/s11668-019-00782-z.

8) Budhe, S., M. D. Banea, M.D. and S. de Barros. 2020. Prediction of the burst pressure for defective pipelines using different semi-empirical models, Frattura ed Integrità Strutturale, 52, pp. 137-147. DOI: 10.3221/IGF-ESIS.52.12.

9) Fu, B.; Kirkwood, M.G. 1995. ''Determination of failure pressure of corroded linepipes using nonlinear finite element method''. In Proceedings of the 2nd International Pipeline Technology Conference, Ostend, Belgium, 11–14 September 1995; Volume II, pp. 1–9.

10) Fu, B.; Batte, A.D. 1999, ''New methods for assessing the remaining strength of corroded pipelines''. In Proceedings of the EPRG/PRCI 12th Biennial Joint Technical Meeting on Pipeline Research, Groningen, The Netherlands, 17–21 May 1999. Paper 28.

11) Netto T.A, Ferraz U.S, Estefen S.F, 2005. The effect of corrosion defects on the burst pressure of pipelines, Journal of Constructional Steel Research, Vol 61, Issue 8, pp 1185-1204. Doi: 10.1016/J.Jcsr.2005.02.010.

12) Bin Ma, Jian Shuai, Dexu Liu, Kui Xu 2013. Assessment on failure pressure of high strength pipeline with corrosion defects, Engineering Failure Analysis, Vol 32, pp 209-219. Doi: 10.1016/J.Engfailanal. 2013.03.015.

13) Zhu. Xian-Kui, Leis. Brian N. 2012. Evaluation of burst pressure prediction models for line pipes, International Journal of Pressure Vessels and Piping, Vol 89, 85-97. Doi: 10.1016/J.Ijpvp.2011.09.007.

14) Olusegun Fatoba, Robert Akid, 2014, ''Low Cycle Fatigue Behaviour of API 5L X65 Pipeline Steel at Room Temperature'', Procedia Engineering, 2014, 74: 279-286, Doi:10.1016/J.Proeng.2014.06.263.

15) Abaqus /CAE 2014, Abaqus Standard /user's manual, Dassault systems, Providence, RI, USA.

16) Shamsuddoha, M., Manalo, A., Aravinthan, T., Islam, M. and Djukic, L. 2021. Failure analysis and design of grouted fibre-composite repair system for corroded steel pipes. Eng. Fail. Anal., 119, 104979. DOI: 10.1016/j.engfailanal.2020.104979.